BMC Microbiology

RESEARCH

Open Access

Eradication of *Helicobacter pylori* reshapes gut microbiota and facilitates the evolution of antimicrobial resistance through gene transfer and genomic mutations in the gut

Meiqi Zhao[1,2†], Yunlong Zhang[3†], Shuangqing Liu[4], Fengmei Wang[2,5] and Peng Zhang[1*]

Abstract

Treating *Helicobacter pylori* (*H. pylori*) infection requires large quantities of antibiotics, thus dramatically promoting the enrichment and dissemination of antimicrobial resistance (AMR) in feces. However, the influence of *H. pylori* eradication on the AMR mobility and the gut microbiota evolution has yet to be thoroughly investigated. Here, a study involving 12 *H. pylori*-positive participants was conducted, and the pre- and post- eradication fecal samples were sequenced. Metagenomic analysis revealed that the eradication treatment drastically altered the gut microbiome, with the *Escherichia* and *Klebsiella* genera emerging as the predominant bacteria. Interestingly, the eradication treatment significantly increased the relative abundance and diversity of resistome and mobilome in gut microbiota. Eradication of *H. pylori* also enriched AMR genes (ARGs) conferring resistance to antibiotics not administered because of the co-location with other ARGs or mobile genetic elements (MGEs). Additionally, the *Escherichia* and *Klebsiella* genera were identified as the primary bacterial hosts of these highly transferable ARGs. Furthermore, the genomic variations associated with ARGs in *Escherichia coli* (*E. coli*) caused by the eradication treatment were profiled, including the *parC*, *parE*, and *gyrA* genes. These findings revealed that *H. pylori* eradication promoted the enrichment of ARGs and MGEs in the *Escherichia* and *Klebsiella* genera, and further facilitated bacterial evolution through the horizontal transfer of ARGs and genomic variations.

Keywords Antimicrobial resistance, Evolution, Gut microbiota, *H. pylori* eradication, Metagenomics

Introduction

Antimicrobial resistance (AMR) has been identified as a major threat to ecological equilibrium and global health; failure to address the growing problem of AMR will result in an annual death of almost 10 million people in the next two decades [1]. Currently, physicians worldwide are confronted with the common predicament that treating infectious diseases requires antibiotics, with no alternative drugs available in clinical settings, as in the treatment of *Helicobacter pylori* (*H. pylori*) infection. This utilization of antibiotics is likely to promote bacterial evolution associated with AMR and facilitates the expansion and diffusion of AMR genes (ARGs) through

†Meiqi Zhao and Yunlong Zhang contributed equally to this work.

*Correspondence:
Peng Zhang
zpeng@email.tjut.edu.cn
[1] Life and Health Intelligent Research Institute, Tianjin University of Technology, Tianjin 300384, China
[2] The Third Central Hospital of Tianjin, Nankai University, Tianjin 300170, China
[3] Hospital of Stomatology, Tianjin Medical University, Tianjin 300070, China
[4] Department of Clinical Laboratory, The Second Hospital of Tianjin Medical University, Tianjin 300211, China
[5] Department of Organ Transplantation, Tianjin Key Laboratory of Organ Transplantation, Tianjin First Central Hospital, Nankai University, Tianjin 300192, China

horizontal transfer in gut bacterial communities [2, 3]. The ongoing evolution of gut bacteria poses a new challenge in the fight against AMR that demands our undivided attention. However, recent studies have primarily concentrated on the alterations of gut bacteria compositions [4, 5], as well as the contamination of known ARGs in bacterial communities [6], the bacterial evolution associated with AMR in gut microbiota induced by *H. pylori* eradication is seldom addressed.

H. pylori, a microaerophilic flagellated bacterium, is estimated to infect approximately half of the world's population and is known to participate in several diseases, such as bad breath, chronic gastritis, peptic ulcer disease, and gastric adenocarcinoma [7–9]. Therefore, eradicating *H. pylori* for treatment or prevention of these disorders is commonly prescribed by physicians, and the recommended eradication regimen requires large quantities of antibiotics for a set duration of time, like the 14-day bismuth-based quadruple therapy [10, 11]. The eradication treatment inevitably leads to an imbalance of the intestinal microbial communities, often accompanied by the proliferation of antibiotic-resistant bacteria and ARGs [12]. However, the influence of *H. pylori* eradication on gut microbiota is far more than that. The horizontal transfer of ARGs associated with antibiotic administration and affiliations of these ARGs still need to be deciphered clearly. These overlooked effects can promote the bacterial evolution associated with AMR, which likely results in serious environmental contamination of ARGs.

The first-line *H. pylori* eradication regimen is the 14-day bismuth-based quadruple therapy, including two types of antibiotics (amoxicillin and clarithromycin), one proton-pump inhibitor, and bismuth. The eradication treatment dramatically declines the alpha diversity, especially species richness, and reduces the proportion of Bacteroidota and Bacillota species [13, 14]. Specifically, the proportion of Pseudomonadota generally increases to very high levels immediately after the eradication treatment [13, 15]. It is worth noting that, following the 14-day bismuth-based quadruple therapy, the relative abundance of ARGs against macrolide and beta-lactam was increased [13]. Upon being discharged into natural environments, these multidrug-resistance bacteria can spread and diffuse ARGs among bacterial communities, resulting in serious threat to ecosystem and even passaging AMR to human-associated pathogens [16].

Twelve *H. pylori*-positive individuals were selected through strict screening in the present study. The fresh fecal samples collected before and immediately after the 14-day bismuth-based quadruple therapy, were sequenced. Reads-based analysis was employed to characterize the alterations of the microbiome, antibiotic resistome, and mobilome in the intestinal community. Additionally, the co-occurrence of ARGs and MGEs was deciphered to determine the bacterial hosts of transferable ARGs. Furthermore, combining comparative genomics and metagenomic intra-species diversity analysis, the phylogenetic relationship of the representative intestinal bacteria (*Escherichia coli*, *E. coli*) was profiled. The genetic variations induced by the eradication treatment were detailed. This study will profile the contamination of ARGs and MGEs in fecal samples from donors subjected to *H. pylori* eradication, reveal potential threat of gut microbiota evolution associated with AMR, and facilitate the comprehensive understanding of the influence of *H. pylori* eradication.

Methods

Study design and participants

We performed a randomized study in 100 *H. pylori*-positive participants suffering from bad breath. These participants were subjected to the eradication treatment with a 14-day bismuth-based quadruple therapy (amoxicillin 1000 mg, clarithromycin 500 mg, rabeprazole 10 mg, and bismuth potassium citrate 220 mg [all given twice daily]). This study was approved by the Institutional Review Board of the Tianjin Third Central Hospital. Written informed consent was obtained from all participants before enrollment. In brief, adult patients (> 20 years) diagnosed with bad breath were eligible, and *H. pylori* infection was confirmed by at least two positive results of rapid urease test, histology, and culture. Participants with any of the following criteria were excluded from this study: (1) previous eradication therapy, (2) allergy to any antibiotic of the study, (3) previous gastrectomy, (4) the coexistence of severe concomitant illness including diseases of metabolic system and gastrointestinal tract, (5) pregnancy or lactation women, (6) the use of antibiotics, proton pump inhibitors, bismuth, within six months, and (7) drinking (> 100 g per week of alcohol) and smoking. And 68 participants were enrolled in our study after the screening. A complete medical history and demographic profiles were obtained from each participant, including age, sex, body weight, body height, medical history, profiles of smoking, alcohol, coffee, and tea consumption once joined the study. Medications were advised to be taken one hour before either breakfast or dinner, and alcohol, probiotic products, and other foods influencing gut microbiota should not be consumed during treatment. To determine the success of eradicating *H. pylori*, a urea breath test was performed six weeks following the eradication treatment. Finally, only 12 participants with successful eradication of *H. pylori*, completed the study according to the strict standards. Fecal samples (10 g) of these participants were taken at homes before and immediately after the eradication treatment. These samples

were dispatched to our laboratory within 4 h of collection and kept at −80 ℃ until they were used.

DNA isolation and metagenomic shotgun sequencing

Microbial DNA was collected from fecal samples with QIAamp PowerFecal Pro DNA Kit (QIAGEN, USA) according to the manufacturer's recommendations. In brief, 100 mg of fecal samples were used to isolate microbial DNA, and the extracted DNA were eluted in a final volume of 50 μL of elution buffer. One μg of microbial DNA was used to prepare DNA libraries with KAPA UDI Adapter Kit (Roche, Switzerland). And the library preparations were sequenced on an Illumina HiSeq platform and 150 bp paired-end reads were generated. Raw sequencing reads were first quality-controlled with Trimmomatic (v0.39) [17], removing adaptors and low-quality reads (read was < 60 bp, contained "N" bases or quality score mean bellow 30). The human genome (GRCh38, GCF_000001405.26) was removed from metagenomic reads using bowtie2 (v2.5.1) [18].

Reads-based profiling of the shotgun metagenomic data

Taxonomic profiling of the shotgun metagenomic data was performed using MetaPhlAn (v4.03) with default parameters, and gut microbiota were quantified at different levels including phylum, family, genus, and species. At the species level, the alpha metrics were calculated to infer species richness, the indices of Shannon and Simpson, and beta diversity was quantified with non-metric multidimensional scaling (NMDS) based on the Bray–Curtis distance. Linear discriminant analysis effect size (LEfSe) was used to identify the differentially abundant taxa before and after the eradication treatment.

To detail the antibiotic resistome in metagenomic data, ARGs-OAP v3.0 was used to annotate the ARG types and subtypes with default settings, and the ARGs were normalized to 16S ribosomal RNA (rRNA) gene. The mobilome was inferred with ARGs-OAP on a well-structured mobile genetic element (MGE) database [19], and the MGEs were also normalized to 16S rRNA gene. The abundances of subtypes of ARGs and MGEs were used to calculate the alpha indices, and the beta diversity was assessed by NMDS on the Bray–Curtis distance.

To explore the relation between gut microbiome, antibiotic resistome, and mobilome, Procrustes analysis was performed in R using the 'vegan' package (v 2.6.4). The Bray–Curtis distance on gut microbiome (species level), antibiotic resistome (subtypes), and mobilome (subtypes), was used as input to the Procrustes analysis. The significance was obtained using the 'protest()' function with 999 permutations. The Spearman's correlation of total abundance of ARGs and MGEs from each donor was determined with 'cor()' function. And the co-occurrence networks were explored using the 'psych' package in R and visualized using Gephi (v0.10.1).

Assembly-based profiling of the shotgun metagenomic data

The postfiltered reads from each donor were individually assembled into contigs with SPAdes (version 3.13.0) [20]. To identify the ARG-containing contig (ACC), Prodigal (V2.6.3) was used to predict the open reading frames (ORFs) within these assembled contigs (> 1000 bp), and the nucleotide sequences of ORFs were searched for ARGs against Structured Antibiotic Resistance Gene database (SARG 3.0) using blastx with an E-value threshold of $1e^{-10}$ [21]. An ORF was identified as an ARG-like sequence based on the criteria of 80% sequence similarity and 70% query coverage [22]. Then, the filtered ACCs were annotated with Kraken2. Finally, to examine the distribution and co-occurrence of ARGs, a manual analysis was conducted to summarize and verify the annotation of ACCs and ARGs on ACCs. To explore the mobility of these ACCs, the nucleotide sequences of filtered ACCs were searched for MGEs against the above MGE database using blastn with an E-value threshold of $1e^{-10}$. An ACC was designated as MGE-containing ACCs with the criteria of 90% sequence similarity and 80% query coverage [23]. The plasmid sequences from assembled contigs (> 1000 bp) were recovered using PlasFlow (V1.1) with default parameters [24].

To decipher the alterations of ARGs (especially the acquired ARGs) induced by *H. pylori* eradication, the metagenome assembly genomes (MAGs) were obtained through metagenome binning using MetaWRAP with default parameters [25]. In brief, these assembled contigs were subjected to bin with the algorithms of MaxBin2 [26], metaBAT2 [27], and CONCOCT [28], and a total of 620 MAGs (bins) were obtained after the bin refinement with the minimum completion to 70% and maximum contamination to 10%. Then, Taxator-tk was used to accurately determine the taxonomy of each bin [29], and PhyloPhlAn (V3.0) was also used to visualize the most prevalent MAGs in these metagenomic samples [30]. The ARGs carried by MAGs were determined using blastx against the SARG database, and a total of 142 ARGs-carrying MAGs were obtained. The maximum-likelihood phylogenetic tree of the 142 MAGs was constructed using PhyloPhlAn (V3.0.3). ResFinder (V4.1) was used to detect the acquired ARGs and AMR-associated chromosomal point mutations in these MAGs [31].

Given to the increasing prevalence and enriched ARGs in *E. coli* after *H. pylori* eradication, we selected this species to explore its genomic evolution. We identified 16 *E. coli* MAGs from all metagenomic samples, and the taxonomy classification was further verified with GTDB-Tk

(v2.1.1) based on GENOME TAXONOMY DATABASE (GTDB) [32]. The maximum likelihood tree of core single nucleotide polymorphisms (SNPs) on these 16 MAGs was identified using kSNP4 [33]. StrainPhlAn was used to extract the reads belonging to *E. coli* (SGB10068) from all metagenomic samples, and compared them with the reference genome in a phylogenetic tree [34].

Isolates of *E. coli* strains and genomic analysis

We randomly isolated *E. coli* strains from the samples of five donors collected before and after the *H. pylori* eradication treatment with the *E. coli*/Coliform Chromogenic Medium (Hopebiol, China). The isolates were verified by PCR targeting 16S rRNA gene (27F: 5′-AGAGTT TGATCCTGGCTCAG-3′ and 1492R: 5′-TACGGYTAC CTTGTTACGACTT-3′) and Sanger sequencing. Subsequently, 20 confirmed *E. coli* clones from one sample were subjected to susceptibility testing using the disk diffusion method. In brief, plates containing Luria Bertani agar were inoculated with bacterial culture adjusted to a turbidity of a 0.5 McFarland, then disks with antibiotics including amoxicillin, clarithromycin, ciprofloxacin, tetracycline, and gentamycin were placed and tightly pressed onto the surfaces of medium. The plates were kept at 37 ℃ for 24 h, and the inhibition zone diameter was measured to assess the antibiotic susceptibility.

We randomly selected the *E. coli* isolates from one donor, then collected the bacterial DNA and performed the whole genome sequencing. Trimmomatic (v0.39) was used to filter poor quality reads (including short reads below 50 bp and N-containing reads) and adaptors from the raw sequencing reads. Then, the high-quality reads were subjected to PanPhlAn 3 for the pangenome-based phylogenomic analysis. To further decipher the genomic mutations in these isolates, bowtie2 (V2.5.1) was used to map these postfiltered reads to the reference genomes of *E. coli* (GCA_000005845.2) [18], bcftools were used to identify variants and manipulate the results [35], integrated genomics viewer (IGV) was used to scrutinize variant calls and bam files manually [36], and TBtools was used to visualize the genomic variations in circos [37]. Given the evolutionary relationship, both *E. coli* strains (isolates 1 & 3 from the pre-eradication sample) were regarded as the initial strains to explore the genomic variations.

To determine the acquired ARGs and AMR-associated chromosomal point mutations, ResFinder (V4.1) was used. Firstly, the contigs of *E. coli* isolates were assembled using SPAdes (version 3.13.0) with '–careful –only-assembler' option [20], and the obtained contigs were subjected to the ResFinder pipeline. The tool of kSNP4 was used to characterize the phylogenetic relationship of these isolates based on SNPs, and iTOL (V6.7.5) was used to visualize the phylogenetic tree [38].

Statistical analysis

Descriptive statistics for all data were manipulated by Excel 2021 (Microsoft Corp., USA). Alpha and beta diversity of taxonomic profiles, ARGs, and MGEs were calculated in the R (v4.2.2), and beta diversity was visualized using non-metric multidimensional scaling (NMDS) with the Bray–Curtis dissimilarity. The Wilcoxon signed-rank test was employed to compare the alpha parameters and genera of gut microbiome from fecal samples collected before and after the *H. pylori* eradication treatment, as well as the antibiotic resistome and mobilome. The Spearman's correlation analysis was finally used to investigate the associations between gut microbiome, antibiotic resistome, and mobilome. A p value of less than 0.05 was regarded as statistically significant. Network visualization was conducted on the interactive platform of Gephi (0.10.1). The phylogenetic tree was plotted with iTOL (V6.7.5) online. The others were all performed in the R or Graphpad Prism 8.

Results

Cohorts of participants

A total of 100 *H. pylori*-positive participants suffering from bad breath were initially screened for the study, and 32 participants were excluded (Fig. 1). Ultimately, only 12 participants, consisting of five men and seven women, completed the entire experiment following the strict standards set forth. Table S1 presents the detailed information on these standard-compliant participants. Fecal samples ($n=24$) were collected before (defined as Cont. group) and after (defined as HPE group) the 14-day *H. pylori* eradication treatment, as in the experiment scheme depicted in Fig. 1.

H. pylori eradication affects gut microbiota composition

The reads-based metagenomic analysis was implemented to profile the gut microbiota alterations induced by the quadruple eradication therapy. Most subjects experienced a significant decrease in species richness, falling below the threshold of 100 immediately after the eradication treatment (Fig. 2a; $p<0.01$). Additionally, both the Shannon and Simpson indices of our subjects were dramatically reduced in the HPE group compared with the baseline microbiota (Cont.) (Fig. 2b, c; $p<0.01$), indicating that most microorganisms had been restrained by *H. pylori* eradication. Furthermore, NMDS analysis based on the Bray–Curtis distances confirmed that the eradication treatment profoundly affected gut microbial composition (Fig. 2d).

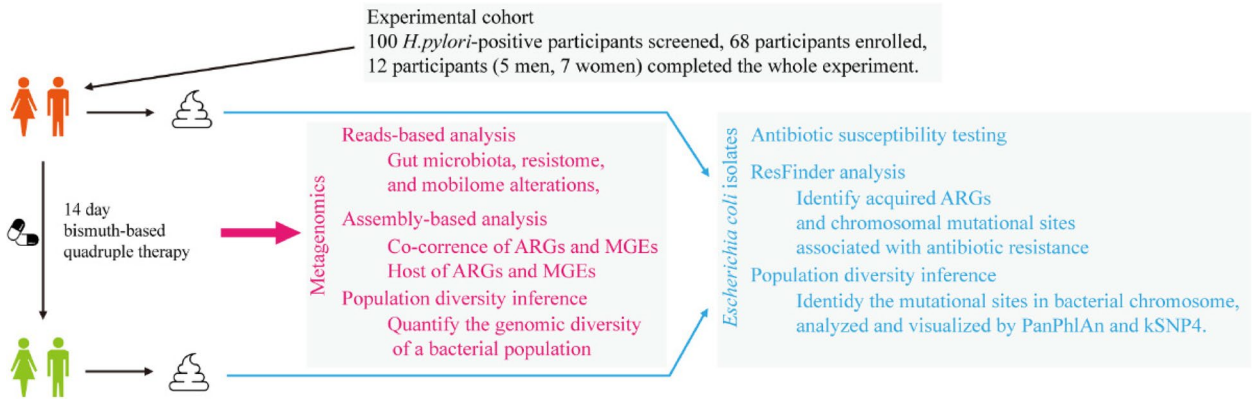

Fig. 1 Schematic visualization of the experimental design

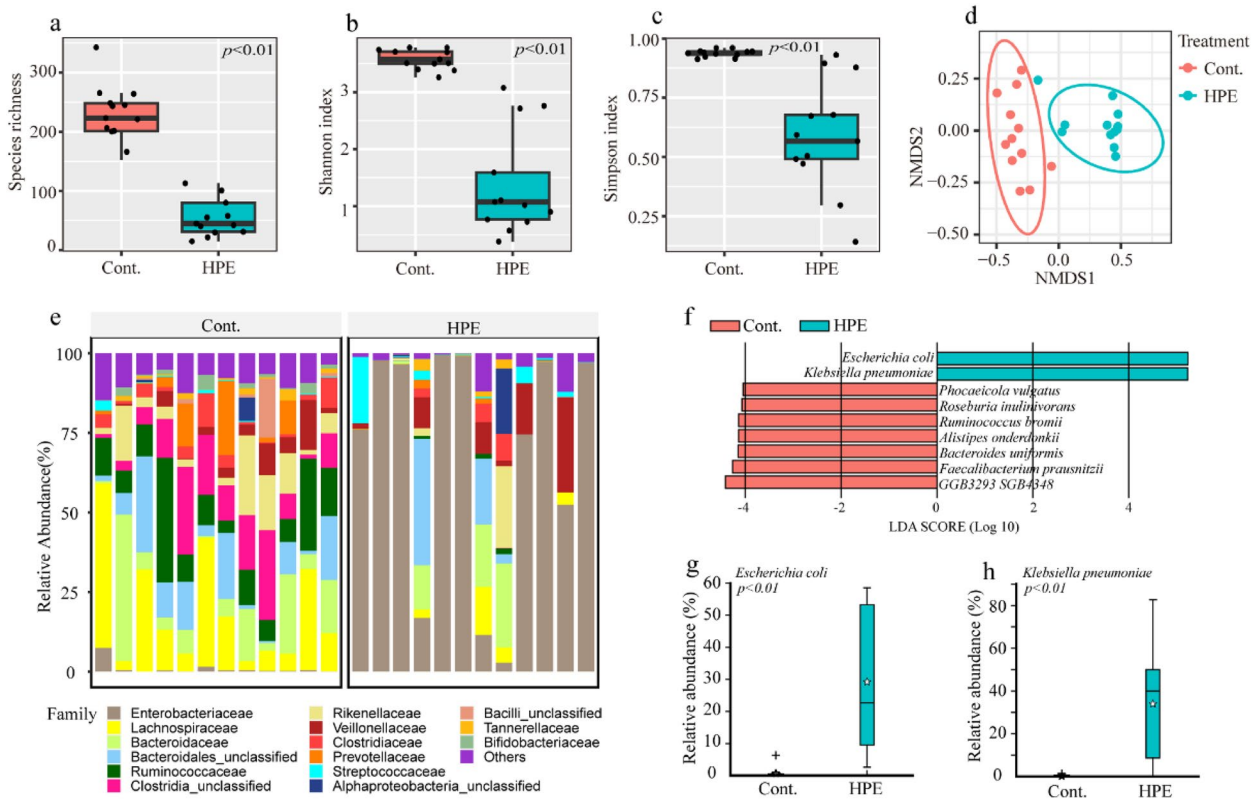

Fig. 2 Structural shift of gut microbiota induced by the *H. pylori* eradication treatment. The microbial community richness (**a**) and alpha diversity, including (**b**) Shannon index and (**c**) Simpson index. **d** NMDS analysis based on the Bray–Curtis distance of bacterial species. **e** The relative abundance of microbial taxa at the family level. **f** The most differentially abundant bacteria species were identified using Lefse analysis, and LDA scores > 4 are shown. The relative abundance of *Escherichia coli* (**g**) and *Klebsiella Pneumoniae* (**h**) in fecal samples collected before and after the *H. pylori* eradication treatment. Cont., samples collected before *H. pylori* eradication; HPE, samples collected immediately after *H. pylori* eradication

It was observed that *H. pylori* eradication had a noticeable influence on gut microbiota at different levels, including phylum, family, and genus (Figs. 2e & S1). Following the eradication treatment, a significant alteration was observed in the predominant phyla of gut microbiota, with a shift from Bacteroidota and Bacillota to Pseudomonadota (Figure S1a). Additionally, the commensal bacteria belonging to the Ruminococcaceae, Lachnospiraceae, Bifidobacteriaceae, Eubacteriaceae, Oscillospira, and Clostridiaceae families were almost eliminated from gut microbiota (Fig. 2e). Notably, the Enterobacteriaceae family was found to be prevalent

among all samples, with a relative abundance exceeding 75% in most subjects. And the eradication treatment significantly altered the relative abundances of 36 bacterial genera (Table S2; $p < 0.05$). Furthermore, the LEFSe results revealed that the *Escherichia* and *Klebsiella* genera were found to be substantially enriched across all donors following the eradication treatment (Fig. 2f), with their average abundance exceeding 30% (Fig. 2g, h; $p < 0.01$). These results reflected that *H. pylori* eradication had profound implications for gut microbiota composition.

H. pylori eradication expands the gut resistome and mobilome

The alterations of ARGs in fecal samples were characterized using the ARGs-OAP pipeline. The Bray–Curtis dissimilarities readily separated the gut resistome of the Cont. and HPE groups (Fig. 3a), and the sum abundance of observed ARGs was sharply increased to a considerable extent (Figure S2a; $p < 0.01$), indicating that the enrichment of ARGs was markedly promoted by *H. pylori* eradication. Additionally, the diversity of ARGs was significantly increased by the eradication treatment, as evidenced by the increased species richness and the Shannon and Simpson indices (Figure S2b-d; $p < 0.01$). Of these, ARGs belonging to beta-lactam and macrolide-lincosamide-streptogramin (MLS) can be directly associated with the antibiotics (amoxicillin and clarithromycin) that were administered in the eradication treatment, including gene *ampC*, *TEM-1*, *TEM-117*, *TEM-193*, *mph(A)*, *erm(B)*, and *erm(F)* (Fig. 3b). Nonetheless, the ARGs that fell under other categories, such as aminoglycoside, multidrug, polymyxin, tetracycline, sulfonamide, and trimethoprim, were also observed to be significantly augmented by the eradication treatment (Fig. 3b). The relative abundances of these ARGs were either equivalent to or higher than those of beta-lactams (Figure S3 and Table S3). The *sul1*, *mph(A)*, *tet(A)*, *dfrA17*, *qacEdelta1*, and *APH(3")-Ib* genes were the most enriched ARGs after the treatment (Table S4).

Previous studies have revealed that the mobilome has a pivotal influence on disseminating ARGs [39]. MGE compositions were analyzed using the well-established MGE database to profile the changes in microbial mobilome induced by *H. pylori* eradication [19]. Consistent with the results of ARGs, the enrichment of MGEs was considerably enhanced by the *H. pylori* eradication treatment, as indicated by the alpha and beta metrics (Figs. 3c and S4; $p < 0.01$). Furthermore, it was found that the relative total abundance of MGEs significantly increased, as evidenced by about a 34-fold change (Fig. 3d). Transposase, IS91, integrase, and plasmid were the predominant categories of MGEs, accounting for approximately 90% of

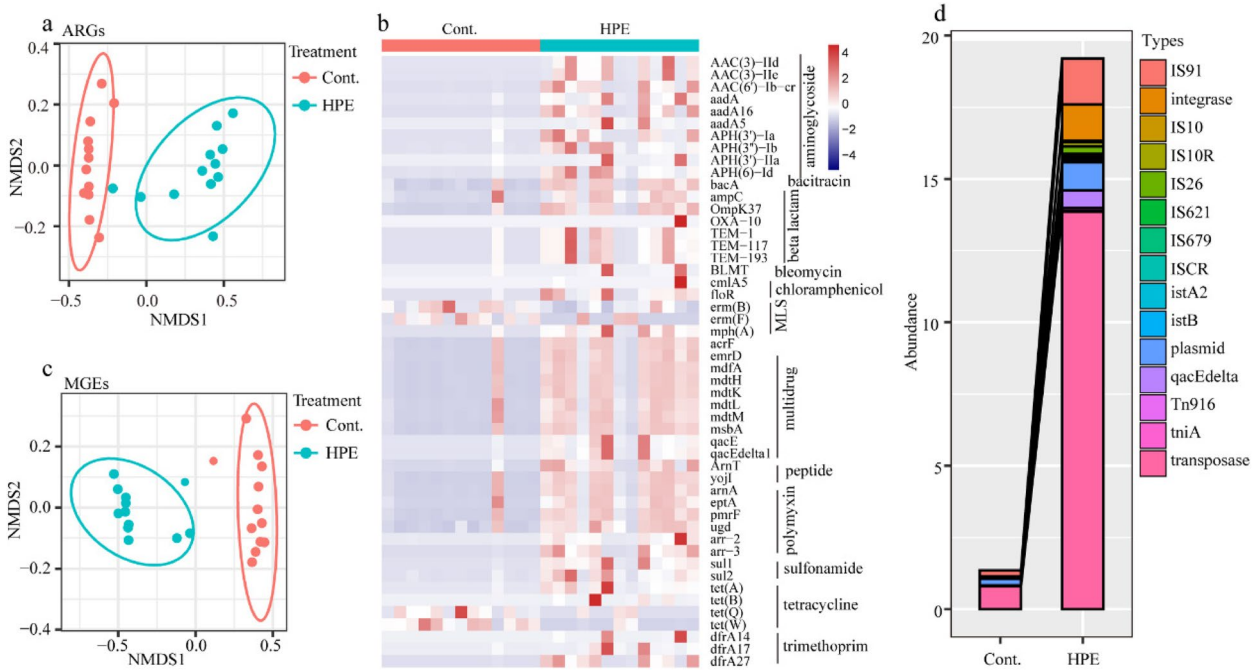

Fig. 3 Fecal resistome and mobilome alterations induced by the *H. pylori* eradication treatment. **a** NMDS analysis based on the Bray–Curtis distance of ARG subtypes. **b** The heatmap of top 50 ARG subtypes. **c** NMDS analysis based on the Bray–Curtis distance of MGE subtypes. **d** The relative abundance of the top 15 MGE types. Cont., samples collected before *H. pylori* eradication; HPE, samples collected immediately after *H. pylori* eradication

the total abundance of MGEs. In detail, the *tnpA*, *IS91*, *intI1*, *qacEdelta*, and *IS26* genes were the most enriched MGEs after *H. pylori* eradication (Figure S5 and Table S5; $p < 0.01$).

H. pylori eradication influences the relations among gut microbiome, resistomes, and mobilomes

The co-occurrence of ARGs and MGEs in specific bacteria, particularly those with pathogenic potential, poses a substantial risk to both ecological equilibrium and human health [19, 40]. The results of Procrustes analysis demonstrated a significant correlation among the resistome, microbiome, and mobilome (Figs. 4a, b and S6; $p < 0.01$) during the *H. pylori* eradication treatment, with decreasing M^2 values indicating a stronger association between the resistome and mobilome ($M^2 = 0.17$). Additionally, the Spearman 's correlation analysis confirmed the notable association between the identified ARGs and MGEs (Fig. 4c; $p < 0.01$). Furthermore, the results of network analysis showed that these ARGs and MGEs had a higher tendency to occur within Enterobacteriaceae species than other bacterial families (Fig. 4d, e), and the predominant bacteria were identified as the *Escherichia* and *Klebsiella* genera. Moreover, it was found that ARGs tended to coexist with MGEs, such as *tnpA*, *IS91*, *intI1*, and *qacEdelta* (Figure S7), indicating a highly transferable potential of these ARGs. These findings suggested that the co-occurrence patterns of resistomes, and

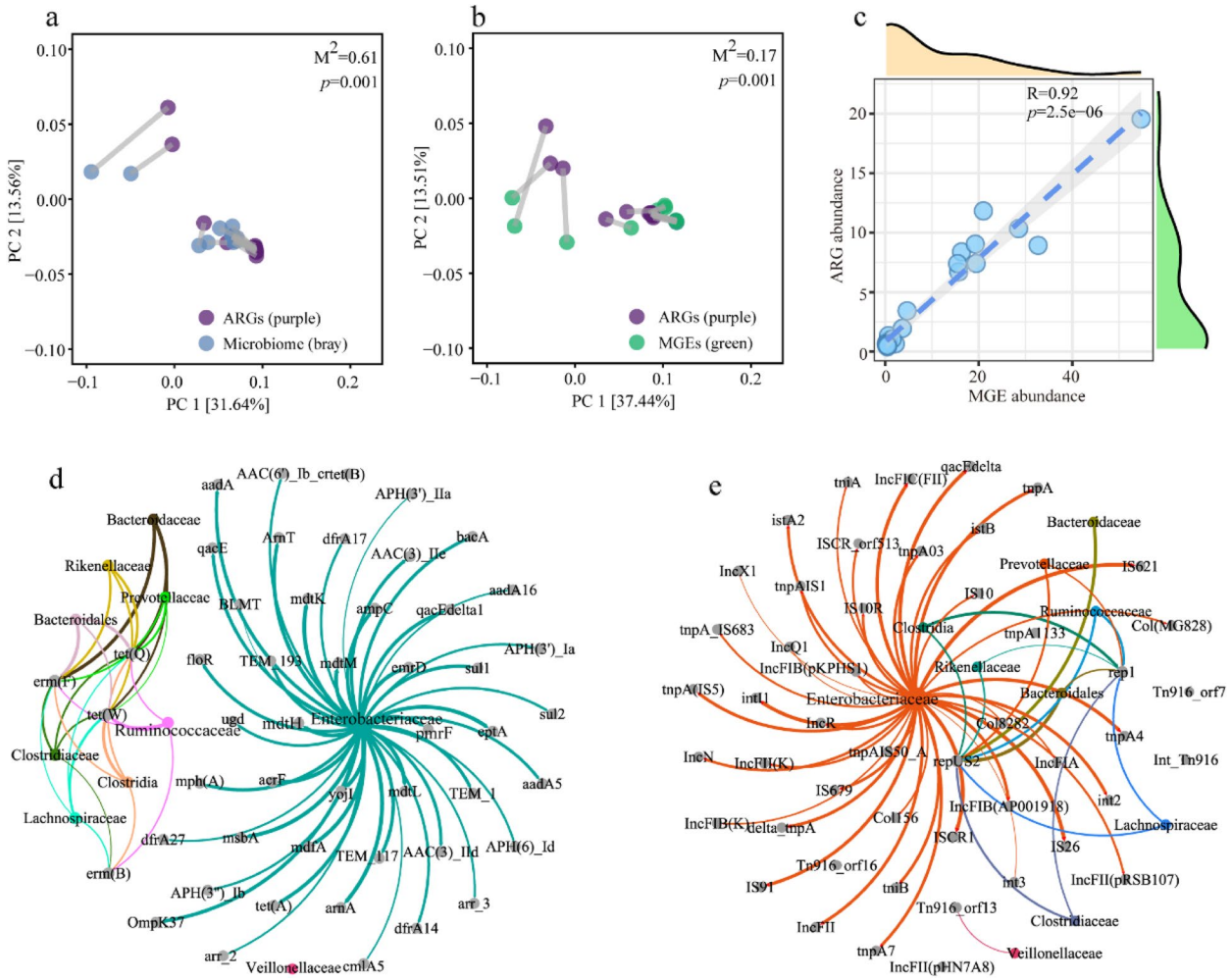

Fig. 4 *H. pylori* eradication influences the relations among microbiomes, resistomes, and mobilomes. The Bray–Curtis distance is determined in the microbiome, ARGs (**a**), and MGEs and ARGs (**b**). Procrustes rotates the results of separate principal coordinates of microbiome (bray symbols), ARGs (purple symbols), and MGEs (green symbols). **c** The Spearman's correlation between the relative total abundance of ARGs and MGEs. The co-occurrence network analysis among the microbiome and ARGs (**d**) and the microbiome and MGEs (**e**). The top 10 bacterial families, top 50 ARG subtypes, and top 50 MGE subtypes are shown. The nodes are colored according to the modularity class, and the number of samples harboring the ARGs is indicated by the weight of curves

microbiome or mobilome were changed by the *H. pylori* eradication treatment.

H. pylori eradication changes the bacterial host composition of ARGs

To further investigate the bacterial hosts of ARGs, an assembly-based metagenomic analysis was implanted, and the ACCs were annotated against KRAKEN2 standard database. Upon analyzing the metagenomic data, a total of 336,176 and 71,039 contigs were obtained from metagenomic samples collected before and after the eradication respectively (Figure S8a). Of these contigs, 783 and 1056 were identified separately as ACCs, and 96.24% of all ACCs were annotated at the phylum level, while 82.49% were annotated at the genus level (Figure S8b, c). Furthermore, the ratio of ACCs showed a remarkable increase from approximately 0.23% to 3.07% after the *H. pylori* eradication treatment (Figure S8d).

Before the eradication of *H. pylori*, the detectable ARGs were predominantly affiliated with 13 families from four phyla, with the most prevalent hosts of ARGs being Bacteroidaceae, Enterobacteriaceae, Lachnospiraceae, and Tannerellaceae (Fig. 5a). Conversely, after the eradication treatment, the majority of ARGs were assigned to Enterobacteriaceae, particularly those associated with MLS, multidrug, beta-lactams, polymyxins, and sulfonamides (Fig. 5b). At the genus level, it was observed that the *Escherichia* and *Klebsiella* genera were the primary hosts of ARGs (Table S6). Moreover, the diversity of ARGs carried by both genera was greater in HPE group than the Cont. group, as represented by these ARGs belonging to aminoglycosides, beta-lactams, and MLS (Figure S9). These results revealed that the enriched ARGs after the *H. pylori* eradication treatment were mainly hosted by the *Escherichia* and *Klebsiella* genera.

Metagenome binning was conducted to confirm the representative hosts of ARGs. After filtering low-quality metagenome-assembled genomes (MAGs), a total of 620 MAGs (> 70% completion and < 10% contamination) were acquired for further investigation. Of these, 508 MAGs were assembled from the metagenomes before *H. pylori* eradication, whereas 112 MAGs were obtained from the post-eradication metagenomes. Subsequently, PhyloPhlAn was employed to visualize the most prominent 22 species-level MAGs (Fig. 5c). The results revealed a wide variety of MAGs in fecal samples before *H. pylori* eradication, with only *E. coli* (16 MAGs, detected in 11/12 donors) and *K. pneumoniae* (eight MAGs, detected in 7/12 donors) being prevalent after *H. pylori* eradication. Furthermore, all MAGs were identified at the species level using the Genome Database Taxonomy (Table S7). Of all MAGs, 142 MAGs were found to harbor ARGs. Before the eradication treatment, 17.7% (90/508) of MAGs contained ARGs in the metagenomes, whereas 46.43% (52/112) of MAGs carried ARGs in the post-eradication metagenomes (Fig. 5d). All 142 ARG-carrying MAGs were combined to conduct the phylogenetic analyses. The results revealed that, after the eradication treatment, the *Escherichia* (11 MAGs), *Klebsiella* (7 MAGs), *Enterococcus* (4 MAGs), and *Streptococcus* (4 MAGs) genera were the predominant ARG-carrying MAGs.

H. pylori eradication facilitates the high transfer potential of AMR

An analysis of plasmid pools was performed using Plasflow to assess the mobility potential of the detectable ARGs. The results demonstrated that more sequences were classified as being carried by plasmids after *H. pylori* eradication (Fig. 6a; $p < 0.01$), indicating a notable enrichment of plasmid in the gut microbiota as a result of the treatment. A thorough investigation was conducted on the identified 1839 ACCs to determine their association with MGEs. The findings revealed a significant increase in the ratio of MGE-carrying ACCs after *H. pylori* eradication, from 4.85% (38/783 ACCs) to 14.58% (154/1056 ACCs; Table S8). Upon analysis, it was observed that the relative abundance of MGE-carrying ACCs significantly increased after *H. pylori* eradication, with the average abundance rising from 8.20% to 44.48% (Fig. 6b; $p < 0.01$). Notably, the ACCs that carried multiple ARGs (≥ two) were seldom identified in the pre-*H. pylori* eradication metagenomes (Table S8). Conversely, after *H. pylori* eradication, the co-occurrence of ARGs and MGEs was commonly observed in metagenomes, and the MGE-carrying ACCs were predominantly hosted by the *Escherichia* and *Klebsiella* genera (Fig. 6c). These ACCs often harbored multiple ARGs, multiple MGE, or both, with the MGEs primarily including *intl1*, *tnpA*, *IS91*, and *aqcEdelta* (Table S8). These results indicated that the emergence of the highly transferable multidrug resistance in gut microbiota was likely facilitated by *H. pylori* eradication.

H. pylori eradication promotes the phenotypic and genotypic evolution of *E. coli* in gut communities

In addition to horizontal gene transfer, genomic mutations are crucial in developing bacterial antibiotic resistance, particularly when exposed to antibiotics. Considering the high prevalence and affiliated ARGs, the research associated with bacterial evolution focused on the *E. coli*. It was found that *E. coli* (SGB10068) was present in only 17 of the 24 metagenomic samples (Fig. 7a). The phylogenetic relationship indicated that this strain's mutation rates (against species-specific MetaPhlAn markers) were much lower before *H. pylori* eradication than after its eradication. Additionally, the evolutionary tendency of *E. coli* strains was validated using the

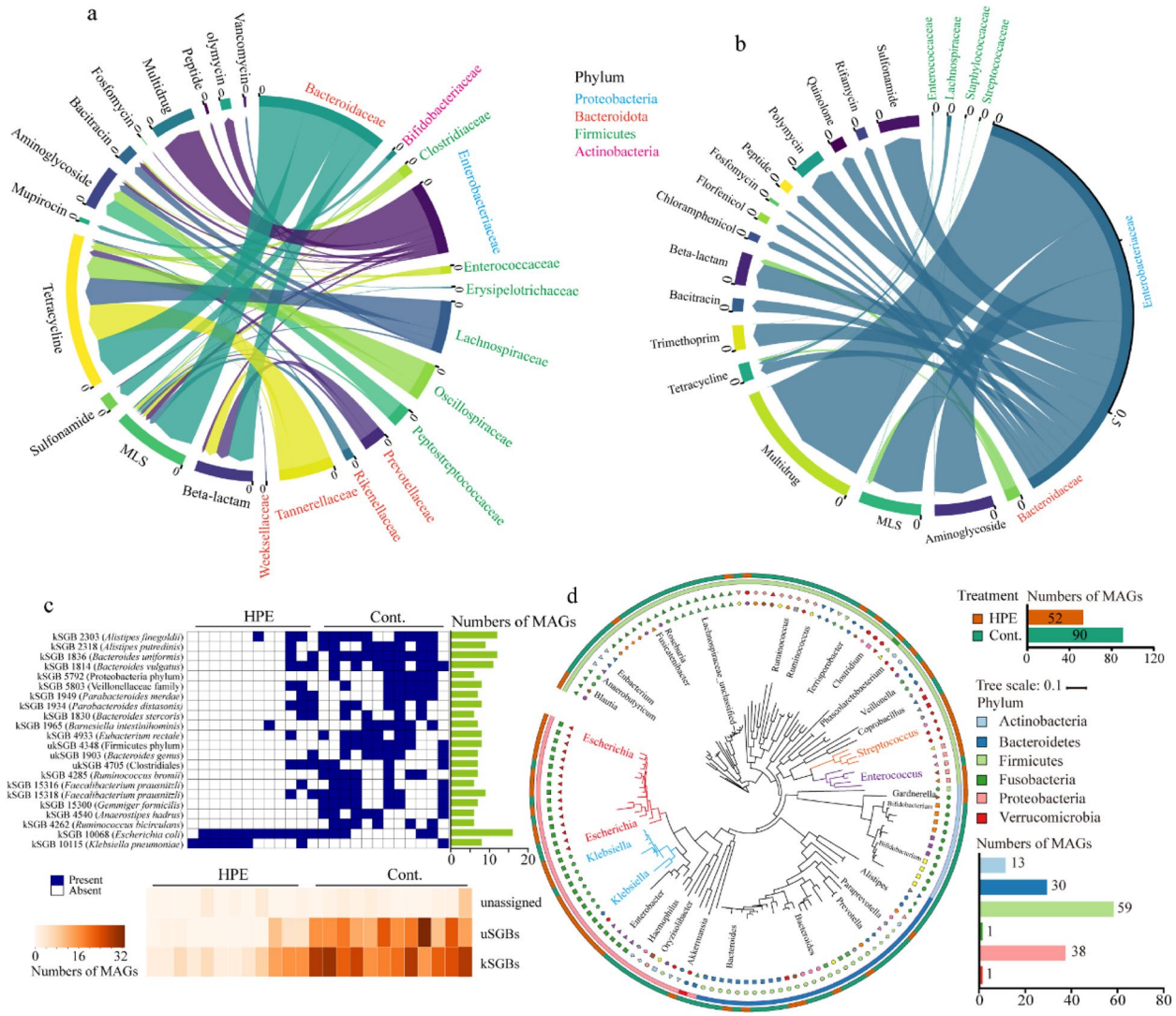

Fig. 5 *H. pylori* eradication changes the compositions of ARG hosts. The mapping relationship between the bacterial families and the carried ARGs across all samples collected before (**a**) and after *H. pylori* eradication (**b**). The mapping relationship between the bacterial families (annotated from the 1056 ACCs) and the carried ARGs across all samples collected after *H. pylori* eradication. In the ACC sector, the percentage of bacterial families is represented by the length of the bars on the inner ring. In the ARGs sector, the percentage of ACCs is represented by the length of the bars on the inner ring. **c** The heatmap of the prevalence profile of the top 22 MAGs annotated using PhyloPhlAn, and the prevalence of uSGBs, kSGBs, and unassigned bins is present in each metagenome. **d** Phylogenetic trees of all 142 ARGs-carrying MAGs affiliated to each family. The maximum-likelihood phylogenetic tree is constructed using PhyloPhlAn; the first three layers indicate the groups of each MAG annotated at species, family, and phylum levels. The groups of each MAG are shown by the outside layer, and MAGs belonging to different groups and families are shown by the histograms in terms of the MAG numbers. ACC, ARG-carrying contig; ARG, antimicrobial resistance gene; MAGs, metagenome-assembled genomes; MLS, Macrolides, lincosamides, streptogramins; uSGBs, unassigned species-level genome bins; and kSGBs, unknown species-level genome bins

phylogenetic relationship predicted on core-genome mutations in the 16 MAGs assigned to this bacterium (Fig. 7b). Moreover, it was discovered that a high occurrence of genomic mutations on the *parC*, *parE*, and *gyrA* genes was exhibited by these *E. coli* MAGs obtained from the post-eradication metagenomes (Figure S10). These mutations are believed to contribute to bacterial resistance to nalidixic acid and ciprofloxacin [41, 42]. However, it is only feasible to identify some of the genomic mutations responsible for antibiotic resistance through metagenomics.

E. coli strains from fecal samples before and after *H. pylori* eradication were randomly isolated to accurately

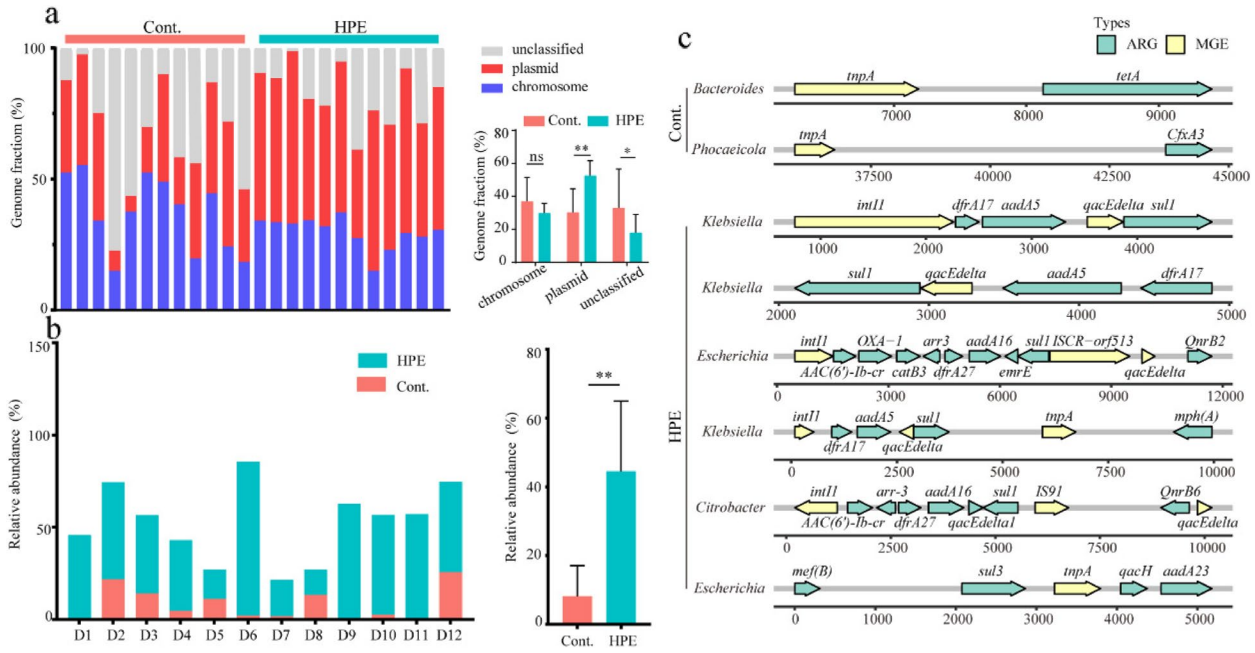

Fig. 6 *H. pylori* eradication boosts the transferable potential of ARGs in gut microbiota. **a** The plasmid in each metagenome is predicted by Plasflow, and the statistical analysis is visualized by histograms on the right. **b** The relative abundance of ACCs between HPE and Cont. for each donor is shown on the left, and the statistical analysis is visualized by histograms on the right. **c** The representative contigs of MGEs-carrying ACCs from the metagenomes before (Cont.) and after (HPE) the HP eradication treatment. Cont., samples collected before *H. pylori* eradication; HPE, samples collected immediately after *H. pylori* eradication. ARG, antimicrobial resistance genes; MGE, mobile genetic element

profile the evolutionary trend. Then, the antibiotic susceptibility of these isolates against five antibiotics (amoxicillin, clarithromycin, ciprofloxacin, tetracycline, and gentamycin) was examined. Most *E. coli* strains isolated after the treatment were resistant to these antibiotics, while the bacterial strains isolated before the treatment showed relatively lower resistance rates (< 20%) (Table S9). Whole genomic sequencing indicated that, a variety of ARGs conferring resistance to aminoglycosides, beta-lactams, macrolides, quinolones, and tetracycline were harbored by the post-eradication isolates (Figure S11). It is likely that *H. pylori* eradication drastically reduced the genetic heterogeneity or diversity within species and promoted the proliferation of antibiotic-resistant clones (Figs. 7c and S11). The results of the phylogenetic relationship based on pan-genome SNPs confirmed that the *H. pylori* eradication treatment likely facilitated the genetic evolution of the surviving *E. coli* strains during the eradication period (Fig. 7d, e). Additionally, genomic variations in genes of *parC*, *parE*, and *gyrA* (Table S10), were in line with the results predicted using ResFinder. Together, these results suggested that the *H. pylori* eradication treatment facilitated intestinal *E. coli* to adapt to antibiotic pressure.

Discussion

To decipher the gut microbiota alteration caused by *H. pylori* eradication, is of great importance to evaluate the influence of the quadruple eradication therapy on the clinical and ecological realms. Prior studies have revealed that *H. pylori* eradication dramatically reduced gut microbiota diversity and facilitated the expansion of ARGs associated with antibiotics administered [13, 14, 43]. However, more research has yet to attempt to identify bacterial hosts of the most prevalent ARGs and to analyze the evolution of these antimicrobial-resistant bacteria, making it difficult to restrain the spread of AMR in the intestinal community and natural environments.

H. pylori-positive participants suffering from bad breath were enrolled in this study to objectively assess the effect of *H. pylori* eradication on gut microbiota. They were provided with a 14-day bismuth-based quadruple therapy. Consistent with previous studies, it was found that the eradication treatment reshaped the intestinal microecology, significantly reducing gut microbiota richness and changing bacterial compositions [14]. This pattern of gut dysbiosis is likely associated with the bactericidal spectrum of amoxicillin and clarithromycin, as Bacteroidota and Bacillota species have been reported to be susceptible to both antibiotics [44, 45]. Bacteroides species were almost eliminated from the intestinal tract,

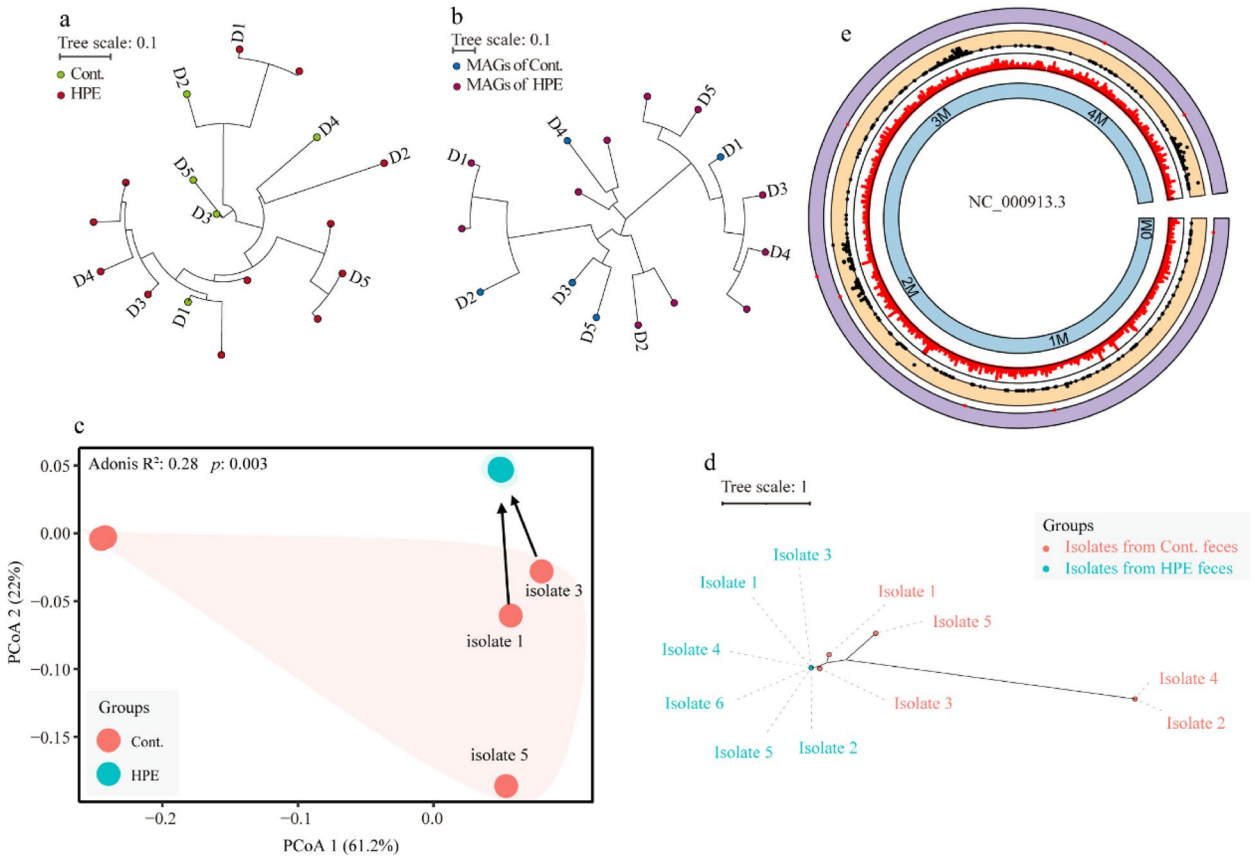

Fig. 7 *H. pylori* eradication promotes the evolution of *E. coli* strains via genomic mutations. **a** Strain-level phylogenetic analysis of *E. coli* identified in the metagenomic samples. The maximum likelihood was used to estimate the phylogenetic tree by applying StrainPhlAn on the raw sequencing reads. **b** The maximum likelihood tree of core SNPs identified using kSNP4 among the 16 *E. coli* MAGs assembled from all metagenomic samples. **c** Principal coordinate analysis on gene presence and absence profiles of the *E. coli* isolates (generated by PanPhlAn). **d** The maximum likelihood phylogenetic tree of core SNPs identified using kSNP4 among the *E. coli* isolates. **e** The locations of the genomic mutations and indels in *E. coli* isolates. From outer to inner rings: the three outermost rings represent locus tag of genes with indels (purple), genes with mutations (orange) and genes density (white), respectively; and the inner ring represents location sites of base in *E. coli* reference genome. Cont., samples collected before *H. pylori* eradication; HPE, samples collected immediately after *H. pylori* eradication

while the species of Bacillota, Actinobacteria, Fusobacteria, and Verrucomicrobia experienced varying levels of decrease in relative abundance. Following the treatment, the proportion of Pseudomonadota increased significantly, with *Escherichia* and *Klebsiella* as the dominant genera, which was mainly due to the enrichment of AMR genes [46]. It is noteworthy that the changes in gut microbiota after the eradication treatment are conflicting in various studies [13–15], which is mainly due to the disparity of baseline microbiota and the antibiotic combinations used [47, 48].

Studies have demonstrated that a prolonged course of antibiotics can significantly increase the presence of ARGs in gut microbiota, especially those that confer resistance to antibiotics administered [5, 49]. The relative abundance of ARGs against β-lactams and macrolides, such as the *mph(A)*, *erm(B)*, *erm(F)*, *TEM-117*, and *TEM-1* genes, was markedly elevated through the eradication treatment with a 14-day bismuth-based quadruple therapy. Of note, *sul1* is the most enriched ARG, which codes for a sulfonamide-resistant dihydropteroate synthase, though no sulfonamide drugs are used in *H. pylori* eradication. This phenomenon is likely caused by the genetic environment in which the *sul1* gene is often connected to other ARGs and transported by class 1 integrons or other MGEs, such as plasmids [50, 51]. In agreement with this, it was also observed that following the eradication of *H. pylori*, the abundance of these ARGs associated with sulfonamide, tetracycline, trimethoprim, and aminoglycoside were remarkably elevated in gut microbiota.

MGEs, including transposons, integrons, and plasmids, are essential for bacterial evolution and the dispersal of cargo such as AMR [52]. These mobile elements

play an instrumental role in the adaptation of bacteria to novel environments, thereby enabling the emergence of distinct bacterial populations [53, 54]. Our findings revealed that the eradication treatment significantly increased the relative total abundance of both ARGs and MGEs, with MGEs having a much higher abundance than ARGs. Transposase, IS91, integrase, and plasmid were the most enriched MGEs, and an increased abundance of plasmid was also confirmed in gut microbiota after the eradication treatment. To profile the correlation between MGEs and ARGs, the co-occurrence and assembly-based metagenomic analyses were conducted. The results demonstrated that the co-location of MGEs and ARGs was commonly observed in gut bacteria after the eradication treatment, and even multiple MGEs and ARGs were often found in one contig. Further analysis verified that the predominant bacterial hosts of these contigs were *Escherichia* and *Klebsiella*. The 14-day bismuth-based quadruple therapy likely facilitated the emergence of multidrug-resistant bacteria, which often harbored highly transferable ARGs. Currently, the prevalence of Enterobacteriaceae in the human gastrointestinal tract is a major concern for clinical practice, and even more so when they have captured transferable multidrug-resistance genes, as this can lead to treatment failure [55, 56]. *Escherichia* has a great capacity to capture accessory genes via horizontal transfer from environments or other bacteria, thus resulting in population diversity and facilitating bacterial evolution [57].

Antibiotic exposure is widely accepted as a major factor in bacteria evolution, especially for acquiring AMR [58]. In addition to gene transfer facilitated by MGEs, genomic variation contributes to obtaining AMR [59]. In this study, the chromosomal point mutations on the *gryA*, *parC*, and *parE* genes in *E. coli* MAGs have been reported to be associated with bacterial resistance to nalidixic acid and ciprofloxacin. The prevalence of these genomic variations in *E. coli* isolates was confirmed through genomic analysis. Furthermore, the evolutionary trend of *E. coli* strains was characterized, and more genomic mutations on genes associated with biofilm formation, biological metabolism, and bacterial response systems were discovered. Interestingly, our findings indicated that long-term antibiotic exposure likely reduced the intraspecific diversity of *E. coli* and promoted the proliferation of these homogeneous strains that contain ARGs.

Nevertheless, there were some limitations to this study. First, after a rigorous screening process, only 12 donors were selected for this study. Second, the metagenomes were just assembled by short-read (150 bp). However, in this study, metagenomic analysis and single bacterial genome analysis were combined to characterize the bacterial host of ARGs and the evolutionary trend of *E. coli*. In addition, the abundance of the *Escherichia* and *Klebsiella* genera in baseline microbiota was insufficient for assembly. Third, fecal samples were just collected from donors before and immediately after the eradication treatment. Further studies are warranted to assess the gut microbiota alterations during the eradication treatment, and fecal samples should be collected on day 0, 3, 7, and 14.

Conclusion

The bismuth-based quadruple therapy markedly affected the microbiome, antibiotic resistome, and mobilome in the gut bacterial community. In addition, the transferable potential of most ARGs was evaluated, and the bacterial hosts of these ARGs were determined. The evolutionary trend of the major drug-resistant bacterium, i.e., *E. coli*, induced by *H. pylori* eradication was analyzed in the present study. These findings raise an alarm that highly transferable ARGs and bacterial evolution of AMR were considerably promoted by drugs in feces, which call for more attention to comprehensively evaluate the influence of the bismuth-based quadruple therapy, as well as to fight against AMR caused by *H. pylori* eradication.

Supplementary Information

The online version contains supplementary material available at https://doi.org/10.1186/s12866-025-03823-w.

Supplementary Material 1

Supplementary Material 2

Acknowledgements
Not applicable.

Financial interests
The authors have no relevant financial or non-financial interests to disclose.

Author's contributions
Peng Zhang and Fengmei Wang designed the research. Meiqi Zhao, Yunlong Zhang, and Shuangqing Liu performed the research. Peng Zhang and Meiqi Zhao analyzed the data. Peng Zhang wrote the paper, with guidance and editing from Fengmei Wang.

Funding
This work was supported by the National Natural Science Foundation of China (No. 32201393).

Data availability
All data, including sequencing data and metadata, used in this manuscript will be freely available to the research community. The sequence data of shotgun metagenomes (24) and E. coli isolates (11) are available on China National Center for Bioinformation (https://ngdc.cncb.ac.cn/gsub), the Accession No. was PRJCA017553. All the codes are available at GitHub: https://github.com/zpeng2022tjut/H.-pylori-eradication.

Declarations

Ethics approval and consent to participate
This study was conducted in accordance with the ethical principles outlined in the Declaration of Helsinki. The ethical permit was reviewed and approved

by the Ethics Committee of Tianjin Third Central Hospital. Written informed consent was obtained from all participants before enrolment.

Consent for publication
Not Applicable.

Competing interests
The authors declare no competing interests.

Received: 7 April 2024 Accepted: 12 February 2025
Published online: 25 February 2025

References

1. Thompson T. The staggering death toll of drug-resistant bacteria. Nature. 2022. https://doi.org/10.1038/d41586-022-00228-x;10.1038/d41586-022-00228-x.
2. San MA. Evolution of plasmid-mediated antibiotic resistance in the clinical context. Trends Microbiol. 2018;26(12):978–85. https://doi.org/10.1016/j.tim.2018.06.007.
3. Roemhild R, Bollenbach T, Andersson DI. The physiology and genetics of bacterial responses to antibiotic combinations. Nat Rev Microbiol. 2022;20(8):478–90. https://doi.org/10.1038/s41579-022-00700-5.
4. Weersma RK, Zhernakova A, Fu J. Interaction between drugs and the gut microbiome. Gut. 2020;69(8):1510–9. https://doi.org/10.1136/gutjnl-2019-320204.
5. Schwartz DJ, Langdon AE, Dantas G. Understanding the impact of antibiotic perturbation on the human microbiome. Genome Med. 2020;12(1):82. https://doi.org/10.1186/s13073-020-00782-x.
6. Thänert R, Sawhney SS, Schwartz DJ, Dantas G. The resistance within: Antibiotic disruption of the gut microbiome and resistome dynamics in infancy. Cell Host Microbe. 2022;30(5):675–83. https://doi.org/10.1016/j.chom.2022.03.013.
7. Robinson K, Atherton JC. The spectrum of helicobacter-mediated diseases. Annu Rev Pathol. 2021;16:123–44. https://doi.org/10.1146/annurev-pathol-032520-024949.
8. Liou JM, Malfertheiner P, Lee YC, Sheu BS, Sugano K, Cheng HC, et al. Screening and eradication of Helicobacter pylori for gastric cancer prevention: the Taipei global consensus. Gut. 2020;69(12):2093–112. https://doi.org/10.1136/gutjnl-2020-322368.
9. Wu Y, Murray GK, Byrne EM, Sidorenko J, Visscher PM, Wray NR. GWAS of peptic ulcer disease implicates Helicobacter pylori infection, other gastrointestinal disorders and depression. Nat Commun. 2021;12(1):1146. https://doi.org/10.1038/s41467-021-21280-7.
10. Zhang W, Chen Q, Liang X, Liu W, Xiao S, Graham DY, et al. Bismuth, lansoprazole, amoxicillin and metronidazole or clarithromycin as first-line Helicobacter pylori therapy. Gut. 2015;64(11):1715–20. https://doi.org/10.1136/gutjnl-2015-309900.
11. Liou JM, Fang YJ, Chen CC, Bair MJ, Chang CY, Lee YC, et al. Concomitant, bismuth quadruple, and 14-day triple therapy in the first-line treatment of Helicobacter pylori: a multicentre, open-label, randomised trial. Lancet (London, England). 2016;388(10058):2355–65. https://doi.org/10.1016/s0140-6736(16)31409-x.
12. Tao ZH, Han JX, Fang JY. Helicobacter pylori infection and eradication: Exploring their impacts on the gastrointestinal microbiota. Helicobacter. 2020;25(6):e12754. https://doi.org/10.1111/hel.12754.
13. Olekhnovich EI, Manolov AI, Samoilov AE, Prianichnikov NA, Malakhova MV, Tyakht AV, et al. Shifts in the Human Gut Microbiota Structure Caused by Quadruple Helicobacter pylori Eradication Therapy. Front Microbiol. 2019;10:1902. https://doi.org/10.3389/fmicb.2019.01902.
14. Hsu PI, Pan CY, Kao JY, Tsay FW, Peng NJ, Kao SS, et al. Helicobacter pylori eradication with bismuth quadruple therapy leads to dysbiosis of gut microbiota with an increased relative abundance of Proteobacteria and decreased relative abundances of Bacteroidetes and Actinobacteria. Helicobacter. 2018;23(4):e12498. https://doi.org/10.1111/hel.12498.
15. Liou J-M, Chen C-C, Chang C-M, Fang Y-J, Bair M-J, Chen P-Y, et al. Long-term changes of gut microbiota, antibiotic resistance, and metabolic parameters after Helicobacter pylori eradication: a multicentre, open-label, randomised trial. Lancet Infect Dis. 2019;19(10):1109–20. https://doi.org/10.1016/s1473-3099(19)30272-5.
16. Rugh MB, Grant SB, Hung WC, Jay JA, Parker EA, Feraud M, et al. Highly variable removal of pathogens, antibiotic resistance genes, conventional fecal indicators and human-associated fecal source markers in a pilot-scale stormwater biofilter operated under realistic stormflow conditions. Water Res. 2022;219:118525. https://doi.org/10.1016/j.watres.2022.118525.
17. Bolger AM, Lohse M, Usadel B. Trimmomatic: a flexible trimmer for Illumina sequence data. Bioinformatics. 2014;30(15):2114–20. https://doi.org/10.1093/bioinformatics/btu170.
18. Langmead B, Salzberg SL. Fast gapped-read alignment with Bowtie 2. Nat Methods. 2012;9(4):357–9. https://doi.org/10.1038/nmeth.1923.
19. Parnanen K, Karkman A, Hultman J, Lyra C, Bengtsson-Palme J, Larsson DGJ, et al. Maternal gut and breast milk microbiota affect infant gut antibiotic resistome and mobile genetic elements. Nat Commun. 2018;9(1):3891. https://doi.org/10.1038/s41467-018-06393-w.
20. Nurk S, Meleshko D, Korobeynikov A, Pevzner PA. metaSPAdes: a new versatile metagenomic assembler. Genome Res. 2017;27(5):824–34. https://doi.org/10.1101/gr.213959.116.
21. Hu Y, Yang X, Qin J, Lu N, Cheng G, Wu N, et al. Metagenome-wide analysis of antibiotic resistance genes in a large cohort of human gut microbiota. Nat Commun. 2013;4:2151. https://doi.org/10.1038/ncomms3151.
22. Ma L, Xia Y, Li B, Yang Y, Li LG, Tiedje JM, et al. Metagenomic assembly reveals hosts of antibiotic resistance genes and the shared resistome in pig, chicken, and human feces. Environ Sci Technol. 2016;50(1):420–7. https://doi.org/10.1021/acs.est.5b03522.
23. Li W, Mao F, Ng C, Jong MC, Goh SG, Charles FR, et al. Population-based variations of a core resistome revealed by urban sewage metagenome surveillance. Environ Int. 2022;163:107185. https://doi.org/10.1016/j.envint.2022.107185.
24. Krawczyk PS, Lipinski L, Dziembowski A. PlasFlow: predicting plasmid sequences in metagenomic data using genome signatures. Nucleic Acids Res. 2018;46(6):e35. https://doi.org/10.1093/nar/gkx1321.
25. Uritskiy GV, DiRuggiero J, Taylor J. MetaWRAP—a flexible pipeline for genome-resolved metagenomic data analysis. Microbiome. 2018;6(1):158. https://doi.org/10.1186/s40168-018-0541-1.
26. Wu YW, Simmons BA, Singer SW. MaxBin 2.0: an automated binning algorithm to recover genomes from multiple metagenomic datasets. Bioinformatics. 2016;32(4):605–7; https://doi.org/10.1093/bioinformatics/btv638.
27. Kang DD, Li F, Kirton E, Thomas A, Egan R, An H, et al. MetaBAT 2: an adaptive binning algorithm for robust and efficient genome reconstruction from metagenome assemblies. PeerJ. 2019;7:e7359. https://doi.org/10.7717/peerj.7359.
28. Alneberg J, Bjarnason BS, de Bruijn I, Schirmer M, Quick J, Ijaz UZ, et al. Binning metagenomic contigs by coverage and composition. Nat Methods. 2014;11(11):1144–6. https://doi.org/10.1038/nmeth.3103.
29. Dröge J, Gregor I, McHardy AC. Taxator-tk: precise taxonomic assignment of metagenomes by fast approximation of evolutionary neighborhoods. Bioinformatics. 2015;31(6):817–24. https://doi.org/10.1093/bioinformatics/btu745.
30. Asnicar F, Thomas AM, Beghini F, Mengoni C, Manara S, Manghi P, et al. Precise phylogenetic analysis of microbial isolates and genomes from metagenomes using PhyloPhlAn 3.0. Nat Commun. 2020;11(1):2500. https://doi.org/10.1038/s41467-020-16366-7.
31. Florensa AF, Kaas RS, Clausen P, Aytan-Aktug D, Aarestrup FM. ResFinder - an open online resource for identification of antimicrobial resistance genes in next-generation sequencing data and prediction of phenotypes from genotypes. Microb Genom. 2022;8(1); https://doi.org/10.1099/mgen.0.000748.
32. Chaumeil PA, Mussig AJ, Hugenholtz P, Parks DH. GTDB-Tk v2: memory friendly classification with the genome taxonomy database. Bioinformatics. 2022;38(23):5315–6. https://doi.org/10.1093/bioinformatics/btac672.
33. Gardner SN, Slezak T, Hall BG. kSNP3.0: SNP detection and phylogenetic analysis of genomes without genome alignment or reference genome. Bioinformatics. 2015;31(17):2877–8; https://doi.org/10.1093/bioinformatics/btv271.

34. Truong DT, Tett A, Pasolli E, Huttenhower C, Segata N. Microbial strain-level population structure and genetic diversity from metagenomes. Genome Res. 2017;27(4):626–38. https://doi.org/10.1101/gr.216242.116.
35. Danecek P, Bonfield JK, Liddle J, Marshall J, Ohan V, Pollard MO, et al. Twelve years of SAMtools and BCFtools. Gigascience. 2021;10(2); https://doi.org/10.1093/gigascience/giab008.
36. Robinson JT, Thorvaldsdottir H, Turner D, Mesirov JP. igv.js: an embeddable JavaScript implementation of the Integrative Genomics Viewer (IGV). Bioinformatics. 2023;39(1); https://doi.org/10.1093/bioinformatics/btac830.
37. Chen C, Chen H, Zhang Y, Thomas HR, Frank MH, He Y, et al. TBtools: An Integrative Toolkit Developed for Interactive Analyses of Big Biological Data. Mol Plant. 2020;13(8):1194–202. https://doi.org/10.1016/j.molp.2020.06.009.
38. Letunic I, Bork P. Interactive Tree Of Life (iTOL) v5: an online tool for phylogenetic tree display and annotation. Nucleic Acids Res. 2021;49(W1):W293–6. https://doi.org/10.1093/nar/gkab301.
39. Carr VR, Shkoporov A, Hill C, Mullany P, Moyes DL. Probing the mobilome: discoveries in the dynamic microbiome. Trends Microbiol. 2021;29(2):158–70. https://doi.org/10.1016/j.tim.2020.05.003.
40. Zhao R, Hao J, Yang J, Tong C, Xie L, Xiao D, et al. The co-occurrence of antibiotic resistance genes between dogs and their owners in families. iMeta. 2022;1(2); https://doi.org/10.1002/imt2.21.
41. Berrazeg M, Jeannot K, Ntsogo Enguéné VY, Broutin I, Loeffert S, Fournier D, et al. Mutations in β-Lactamase AmpC increase resistance of pseudomonas aeruginosa isolates to antipseudomonal cephalosporins. Antimicrob Agents Chemother. 2015;59(10):6248–55. https://doi.org/10.1128/aac.00825-15.
42. Cho H, Misra R. Mutational activation of antibiotic-resistant mechanisms in the absence of major drug efflux systems of escherichia coli. J Bacteriol. 2021;203(14): e0010921. https://doi.org/10.1128/jb.00109-21.
43. Hsu PI, Pan CY, Kao JY, Tsay FW, Peng NJ, Kao SS, et al. Short-term and long-term impacts of Helicobacter pylori eradication with reverse hybrid therapy on the gut microbiota. J Gastroenterol Hepatol. 2019;34(11):1968–76. https://doi.org/10.1111/jgh.14736.
44. Kumar S, Raj VS, Ahmad A, Saini V. Amoxicillin modulates gut microbiota to improve short-term high-fat diet induced pathophysiology in mice. Gut Pathog. 2022;14(1):40. https://doi.org/10.1186/s13099-022-00513-0.
45. Nel Van Zyl K, Matukane SR, Hamman BL, Whitelaw AC, Newton-Foot M. Effect of antibiotics on the human microbiome: a systematic review. Int J Antimicrob Agents. 2022;59(2):106502; https://doi.org/10.1016/j.ijantimicag.2021.106502.
46. Hetzer B, Orth-Höller D, Würzner R, Kreidl P, Lackner M, Müller T, et al. "Enhanced acquisition of antibiotic-resistant intestinal E. coli during the first year of life assessed in a prospective cohort study". Antimicrobial resistance and infection control. 2019;8:79; https://doi.org/10.1186/s13756-019-0522-6.
47. Rashidi A, Ebadi M, Rehman TU, Elhusseini H, Nalluri H, Kaiser T, et al. Gut microbiota response to antibiotics is personalized and depends on baseline microbiota. Microbiome. 2021;9(1):211. https://doi.org/10.1186/s40168-021-01170-2.
48. Wastyk HC, Fragiadakis GK, Perelman D, Dahan D, Merrill BD, Yu FB, et al. Gut-microbiota-targeted diets modulate human immune status. Cell. 2021;184(16):4137-53.e14. https://doi.org/10.1016/j.cell.2021.06.019.
49. Carvalho MJ, Sands K, Thomson K, Portal E, Mathias J, Milton R, et al. Antibiotic resistance genes in the gut microbiota of mothers and linked neonates with or without sepsis from low- and middle-income countries. Nat Microbiol. 2022;7(9):1337–47. https://doi.org/10.1038/s41564-022-01184-y.
50. Koczura R, Mokracka J, Taraszewska A, Łopacinska N. Abundance of Class 1 integron-integrase and sulfonamide resistance genes in river water and sediment is affected by anthropogenic pressure and environmental factors. Microb Ecol. 2016;72(4):909–16. https://doi.org/10.1007/s00248-016-0843-4.
51. de Los SE, Laviña M, Poey ME. Strict relationship between class 1 integrons and resistance to sulfamethoxazole in Escherichia coli. Microb Pathog. 2021;161(Pt A):105206. https://doi.org/10.1016/j.micpath.2021.105206.
52. Botelho J, Schulenburg H. The role of integrative and conjugative elements in antibiotic resistance evolution. Trends Microbiol. 2021;29(1):8–18. https://doi.org/10.1016/j.tim.2020.05.011.
53. Hall JPJ, Harrison E, Baltrus DA. Introduction: the secret lives of microbial mobile genetic elements. Philos Trans R Soc Lond B Biol Sci. 1842;2022(377):20200460. https://doi.org/10.1098/rstb.2020.0460.
54. Zhang Q, Rho M, Tang H, Doak TG, Ye Y. CRISPR-Cas systems target a diverse collection of invasive mobile genetic elements in human microbiomes. Genome Biol. 2013;14(4):R40. https://doi.org/10.1186/gb-2013-14-4-r40.
55. Zahar JR, Blot S, Nordmann P, Martischang R, Timsit JF, Harbarth S, et al. Screening for Intestinal Carriage of Extended-spectrum Beta-lactamase-producing Enterobacteriaceae in Critically Ill Patients: Expected Benefits and Evidence-based Controversies. Clin Infect Dis. 2019;68(12):2125–30. https://doi.org/10.1093/cid/ciy864.
56. Denamur E, Clermont O, Bonacorsi S, Gordon D. The population genetics of pathogenic Escherichia coli. Nat Rev Microbiol. 2021;19(1):37–54. https://doi.org/10.1038/s41579-020-0416-x.
57. Wu S, Tian P, Tan T. Genomic landscapes of bacterial transposons and their applications in strain improvement. Appl Microbiol Biotechnol. 2022;106(19–20):6383–96. https://doi.org/10.1007/s00253-022-12170-z.
58. Bakkeren E, Diard M, Hardt WD. Evolutionary causes and consequences of bacterial antibiotic persistence. Nat Rev Microbiol. 2020;18(9):479–90. https://doi.org/10.1038/s41579-020-0378-z.
59. Verstraete L, Van den Bergh B, Verstraeten N, Michiels J. Ecology and evolution of antibiotic persistence. Trends Microbiol. 2022;30(5):466–79. https://doi.org/10.1016/j.tim.2021.10.001.

Publisher's Note